

## OPTICAL AND MÖSSBAUER SPECTROSCOPY STUDIES ON $\text{YVO}_4:\text{Eu}$ NANOPHOSPHOR

A. M. VOICULESCU<sup>1\*</sup>, E. COTOI<sup>1</sup>, O. TOMA<sup>1</sup>, S. GEORGESCU<sup>1</sup>,  
S. CONSTANTINESCU<sup>2</sup>, I. BIBICU<sup>2</sup>

<sup>1</sup>National Institute for Laser, Plasma and Radiation Physics, Magurele, Romania

<sup>2</sup>National Institute for Materials Physics, Magurele, Romania

\*corresponding author: E-mail: ana.chinie@inflpr.ro

(Received May 25, 2009)

*Abstract.* Using europium as sensitive probe for both fluorescence and Mössbauer spectroscopy the morphological changes (local symmetry, covalence, ionicity) induced by the thermal treatments in the  $\text{YVO}_4$  nanocrystals (synthesized by direct precipitation method) are put into evidence.

*Key words:*  $\text{YVO}_4$ , nanopowders,  $\text{Eu}^{3+}$ , fluorescence, Mössbauer spectroscopy.

### 1. INTRODUCTION

$\text{YVO}_4:\text{Eu}$  is a strongly luminescent material which has been used as the red phosphor in cathode ray tubes for more than 20 years [1-3].

The crystalline  $\text{YVO}_4$  adopts the tetragonal structure (space group of  $I4_1/amd$ ) composed of  $\text{YO}_8$  dodecahedra (the point symmetry of  $\text{Y}^{3+}$  is  $D_{2d}$ ) and  $\text{VO}_4$  tetrahedra (symmetry  $D_{2d}$ ). The rare earth ions occupy the  $\text{Y}^{3+}$  site in  $\text{YVO}_4$  [4].

In this paper,  $\text{YVO}_4:\text{Eu}$  nanocrystalline powders synthesized by direct precipitation method and annealed at various temperatures are characterized by optical and Mössbauer spectroscopy.

### 2. EXPERIMENTAL

The  $\text{Y}_{0.95}\text{Eu}_{0.05}\text{VO}_4$  powder was synthesized by direct precipitation reaction [5]. A mixture of two solutions ( $\text{Y}(\text{NO}_3)_3$  and  $\text{Eu}(\text{NO}_3)_3$ ) was added to a solution of  $\text{NH}_4\text{VO}_3$  whose pH was adjusted to 12.5 with NaOH. The obtained colloid was heated at  $60^\circ\text{C}$  for one hour under magnetic stirring. The nanocrystals were separated from the solution by filtering and then dried at  $60^\circ\text{C}$ .

The resulting powders were annealed at  $300^\circ\text{C}$ ,  $400^\circ\text{C}$ ,  $500^\circ\text{C}$ ,  $550^\circ\text{C}$ ,  $600^\circ\text{C}$ , and,  $900^\circ\text{C}$  for four hours in air.

The fluorescence spectra were recorded using a setup with a Xenon lamp with suitable filters as pumping source, a Jarrel-Ash monochromator (1 m) equipped with an S-20 photomultiplier, and a lock-in amplifier (SR 830) online with a PC. The fluorescence signal was modulated with a SR 540 chopper.

The Mössbauer spectra (MS) were carried out in the standard transmission geometry, using  $^{151}\text{Eu}$  isotope in  $\text{Eu}_2\text{O}_3$  matrix as Mössbauer source of initial activity of 100 mCi. The velocity range was  $\pm 24$  mm/s and saw-tooth velocity function was used. The energy scale was determined using  $\text{Fe}_2\text{O}_3$  and  $\text{Eu}_2\text{O}_3$  etalons.

### 3. RESULTS AND DISCUSSION

#### 3.1. Fluorescence measurements

The transition  ${}^5D_0 \rightarrow {}^7F_1$  of  $\text{Eu}^{3+}$  is a pure magnetic-dipole transition, allowed by the parity selection rule. Its probability can be calculated provided that the free ion wavefunctions are known. This transition is practically insensitive to the changes in the neighborhood of the  $\text{Eu}^{3+}$  ion and is used as an internal standard [6-8]. The electric dipole transition  ${}^5D_0 \rightarrow {}^7F_2$  is very sensitive to the structural changes (hypersensitive transition) [9]. It is a common practice to use the ratios  $R_2 = \text{area}({}^5D_0 \rightarrow {}^7F_2) / \text{area}({}^5D_0 \rightarrow {}^7F_1)$  and  $R_4 = \text{area}({}^5D_0 \rightarrow {}^7F_4) / \text{area}({}^5D_0 \rightarrow {}^7F_1)$  to obtain structural information about the luminescence centres. In Fig. 1, the areas of these transitions are marked for an  $\text{YVO}_4:\text{Eu}^{3+}$  sample annealed at  $900^\circ\text{C}$ .

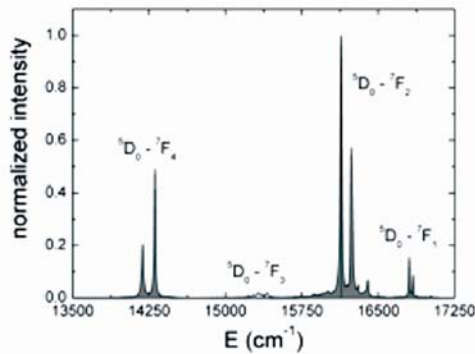


Fig. 1 – Fluorescence spectrum (transitions  ${}^5D_0 \rightarrow {}^7F_{1,2,3,4}$ ) for a  $\text{YVO}_4:\text{Eu}$  sample annealed at  $900^\circ\text{C}$ .

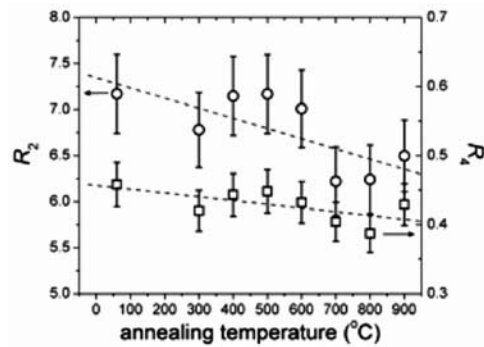


Fig. 2 – The ratios  $R_2, R_4$  of the intensities of the electric- and magnetic-dipole transitions function of the annealing temperature. The dashed lines merely suggest the decrease of both  $R_2$  and  $R_4$ .

The dependence of the ratios  $R_{2,4}$  on the annealing temperature is presented in Fig. 2. The dependence of  $R_2$  with the increasing of the annealing temperature denotes an increase of the local symmetry and or the decrease of the covalence of the  $\text{Eu}^{3+}-\text{O}^{2-}$  bonding. The interpretation of the behavior of  $R_4$  is less straight-

forward. According to [10] it can be associated with the rigidity of the host of the rare earth ion, while [11] relates it to long-range effects (related to bulk properties of the host).

### 3.2. Mössbauer measurements

The  $^{151}\text{Eu}:\text{YVO}_4$  Mössbauer spectra obtained at room temperature for the investigated samples are characterized by a low value of the ratio  $r$  between square deviation of the normalized background and effect (relative deep of the resonance)  $r = \varepsilon/\text{SDF} \cong 0.6$ .

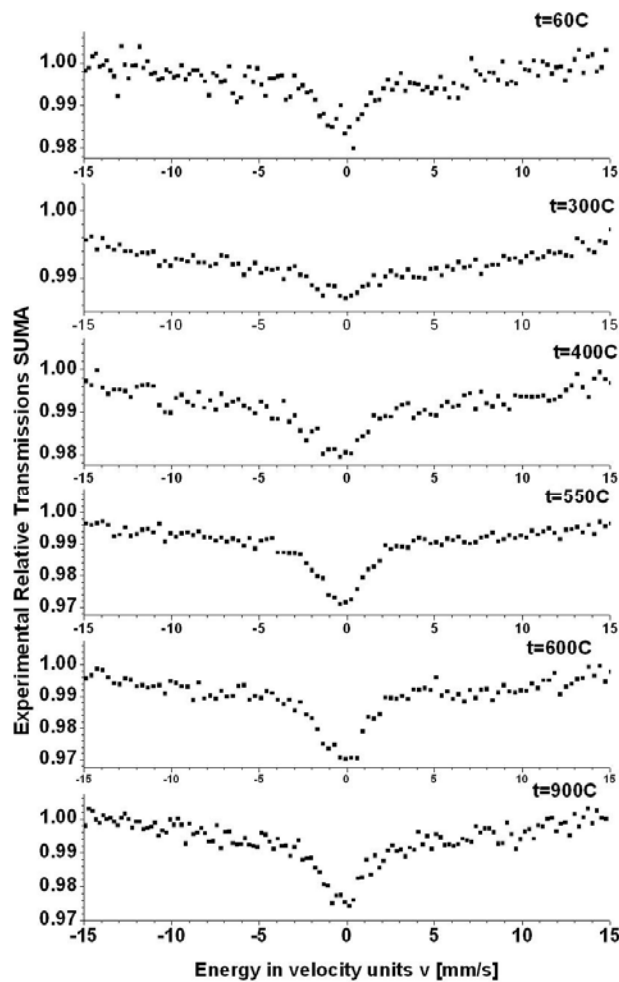


Fig. 3 – The experimental Mössbauer spectra of  $\text{YVO}_4\text{:Eu}$  powders annealed at various temperatures.

The experimental and fitted spectra are plotted in Figs. 3 and 4. In the Table 1 the hyperfine spectrum parameters extracted from the fitting procedure applied to the spectra are given. The  $\chi^2$  criterion was used in the fitting procedure [12].

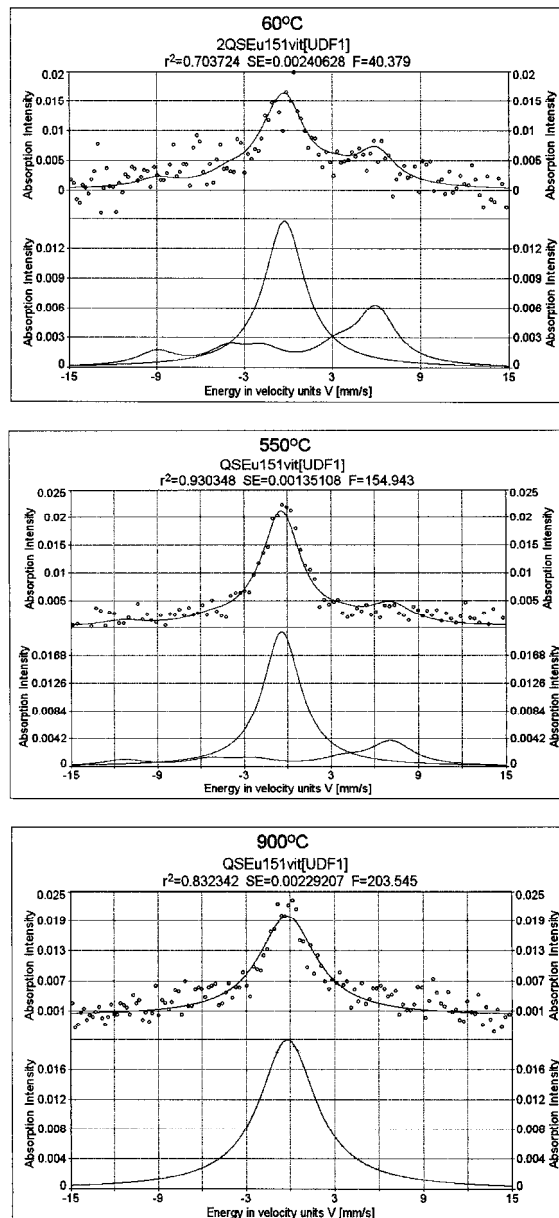


Fig. 4 – Some examples of fitted Mössbauer spectra.

The line shapes of each spectrum evidence a central asymmetric deep at  $\nu \cong 4\text{-}5$  mm/s for ‘as prepared’ sample (dried at  $60^\circ\text{C}$ ) as well as for the annealed samples at temperatures lower than  $900^\circ\text{C}$ . The spectra of the ‘as prepared’ sample and of the samples annealed at  $550^\circ\text{C}$  and  $600^\circ\text{C}$  were fitted with two superimposed elementary patterns (called A- and B-pattern) suggesting two different micro-environments of  $^{151}\text{Eu}$ . The best fit was obtained for quadrupolar patterns, denoting the presence of an electric field gradient (EFG) of the crystal field at the Mössbauer nuclide site [12, 13]. The central shifts of both elementary patterns correspond to trivalent europium [14]. The values of A-patterns evidence a more ionic chemical bonding Eu-O than for B-patterns. Moreover, the values of the quadrupolar parameters are higher for B-patterns, denoting a more distorted Eu-surroundings and higher EFG for B sites.

The half linewidths of the elementary patterns resonances are in the theoretical limits,  $\Gamma_{\text{obs}} \in [1.35 \div 2.2]$  mm/s, corresponding to well-defined A and B micro-environments. But, generally,  $\Gamma_{\text{obs,B}} > \Gamma_{\text{obs,A}}$  could be observed, denoting a different paramagnetic spin-relaxation for the Eu in the two sites, (slower paramagnetic spin-relaxation for Eu in B sites than for A sites) at room temperature. Generally, the half-linewidth of the first elementary pattern is constant and also one remarks the highest value of  $\Gamma_{\text{obs,B}}$  for the sample annealed at  $550^\circ\text{C}$ . This suggests the presence of some other dynamic processes before the extension of the second micro-environment. The spectrum of the sample annealed at  $900^\circ\text{C}$  has the best fit for one pattern only, with hyperfine parameters values much closed to A-parameters values for other samples. The higher value of  $\Gamma_{\text{obs}}$  for the sample annealed at  $900^\circ\text{C}$  denotes an intense paramagnetic spin interaction. The fitted relative areas evidence a decreasing trend of the B patterns.

Table 1

The values of the hyperfine parameters

Annealing temperature	Elementary Pattern	Central Shift $\delta_{\text{c}}$ [mm/s]	Quadrupolar parameter $eQ_{7/2}V_{\text{ZZ}}$ [mm/s]	Half-linewidth $\Gamma_{\text{obs}}$ [mm/s]	Relative Area a [%]
60	A	-0.24	-0.33	1.69	56.85
	B	0.90	69.81	1.60	43.15
550	A	-0.34	0.00	1.60	70.47
	B	0.89	86.32	1.78	29.53
600	A	-0.32	9.46	1.58	69.21
	B	0.98	87.29	1.66	30.79
900	A	-0.20	-0.05	2.35	100
Errors	$\pm 0.07$	$\pm 0.21$	$\pm 0.07$	$\pm 2.5\%$	

The Mössbauer results suggest that two environments correspond to the signal of the  $^{151}\text{Eu}$  - grain core (A-pattern) and on the grain surface (B patterns). As

Eu<sup>3+</sup> substitutes Y<sup>3+</sup> in YVO<sub>4</sub> micro-crystals, A-pattern corresponds to symmetric oxygen-surrounding of <sup>151</sup>Eu and B-pattern corresponds to a very asymmetric one, close to particle surface. The growth of the particles will diminish the surface contribution to spectrum and the volume contribution becomes dominant at the annealing temperature of 900°C.

#### 4. CONCLUSIONS

Optical fluorescence and Mössbauer spectroscopy were used to monitor the evolution with annealing temperature of YVO<sub>4</sub>:Eu nanocrystals synthesized by direct precipitation method.

The intensity ratios  $R_2=I(^5D_0 \rightarrow ^7F_2)/I(^5D_0 \rightarrow ^7F_1)$  and  $R_4=I(^5D_0 \rightarrow ^7F_4)/I(^5D_0 \rightarrow ^7F_1)$  decrease with the increase the annealing temperature, denoting an increase of the local symmetry and an improvement of the ‘bulk’ properties.

The analysis of the experimental <sup>151</sup>Eu Mössbauer spectra evidenced: (i) the spectra are located around 0 mm/s denoting that the valence state of Eu in YVO<sub>4</sub> is +3; (ii) two subsystems (A, B) can be distinguished in the spectrum of the sample annealed at 600°C, corresponding to the two different quadrupolar interaction <sup>151</sup>Eu probe – surroundings; (iii) the two subsystems have close values of the half-linewidths and the areas, very different values of the quadrupolar parameters; (iv) the subsystem B with the higher value of the quadrupolar parameter is shifted to the positive velocity values, relative to the subsystem A (see the Table 1); (v) a single subsystem can be distinguished in the spectrum of the sample annealed at 900°C. We consider that the subsystem A could be associated to the grain core while the subsystem B to the grain surface.

*Acknowledgement.* This work was supported in part from the CEEX 05-D11-07 project of the Romanian National Authority for Scientific Research.

#### REFERENCES

1. C. Brecher, H. Samelson, A. Lempicki, R. Riley, T. Peters, *Polarized Spectra and Crystal-Field Parameters of Eu<sup>3+</sup> in YVO<sub>4</sub>*, *Phys.Rev.*, **155**, 178–187 (1967).
2. A. K. Levine, F. C. Palilla, *A new, highly efficient red-emitting cathodoluminescent phosphor (YVO<sub>4</sub>:Eu) for color television*, *Appl. Phys. Lett.*, **5**, 118–120 (1964).
3. F. C. Palilla, A. K. Levine, *YVO<sub>4</sub>:Eu a Highly efficient, Red-Emitting Phosphor for High Pressure Mercury Lamps*, *Applied Optics*, **5**, 1467–1468 (1966).
4. J. A. Baglio, O. J. Sovers, *Crystal Structures of the Rare-Earth Orthovanadates*, *J. Sol. St. Chem.*, **3**, 458–465 (1971).
5. Y. Li, G. Hong, *Synthesis and luminescence properties of nanocrystalline YVO<sub>4</sub>:Eu<sup>3+</sup>*, *J. Sol. State Chem.*, **178**, 645–649 (2005).
6. R. Reisfeld, E. Zigansky, M. Gaft, *Europium probe for estimation of site symmetry in glass films, glasses and crystals*, *Mol. Phys.*, **102**, 1319–1330 (2004).

7. C. Görrler-Walrand, L. Fluyt, A. Ceulemans, *Magnetic dipole transitions as standards for Judd-Ofelt parametrization in lanthanide spectra*, J. Chem. Phys., **95**, 3099–3106 (1991).
8. P. Babu, C. K. Jayasankar, *Optical spectroscopy of Eu<sup>3+</sup> ions in lithium borate and lithium fluoroborate glasses*, Physica B, **279**, 262–281 (2000).
9. C. K. Jørgensen, B. R. Judd, *Hypersensitive pseudoquadrupole transitions in lanthanides*, Mol. Phys., **8**, 281–290 (1964).
10. H. Takebe, K. Morinaga, T. Izumitani, *Correlation between radiative transition probabilities of rare-earth ions and composition in oxide glasses*, J. Non-Crystalline Solids, **178**, 58–63 (1994).
11. E. W. J. L. Oomen, A. M. A. van Dongen, *Europium (III) in oxide glasses Dependence of the emission spectrum upon glass composition*, J. Non-Crystalline Solids, **111**, 205–213 (1989).
12. D. Barb, *Grundlagen und anwendungen der Mössbauerspektroskopie*, Akademie-Verlag, 1980.
13. S. Ofer, I. Nowik, S. G. Cohen, *The Mössbauer effect in rare earths and their compounds*, in: *Chemical Applications of Mössbauer Spectroscopy*, eds. V. I. Golanskii and R. H. Herber, Academic Press, New York, 1968, 427–503.
14. N. N. Greenwood, T. C. Gibb, *Mössbauer Spectroscopy*, Chapman and Hall Ltd., London, 1971, pp. 543–555.